

Synthesis, Structure, and Properties of Di- μ -phenoxo-bridged Dinuclear Cu^{II}Ni^{II} and Cu^{II}Co^{II} Complexes and Cyclic Di- μ -phenoxo- μ -amido-bridged Tetranuclear Cu₂^{II}Zn₂^{II} and Cu₄^{II} Complexes Derived from the 1,2-Bis(2-oxidobenzamidato)benzenecuprate(II) Dianionic Ligand-Complex

Yukinari Sunatsuki,[‡] Toshihiro Matsuo, Masaaki Nakamura, Fumiaki Kai, Naohide Matsumoto,* and Jean-Pierre Tuchagues[†]

Department of Chemistry, Faculty of Science, Kumamoto University, Kurokami 2-39-1, Kumamoto 860-8555

[‡]Laboratoire de Chimie de Coordination du CNRS, UP 8241 liée par conventions à l'Université Paul Sabatier et à l'Institut National Polytechnique, 205 route de Narbonne, 31077 Toulouse Cedex, France

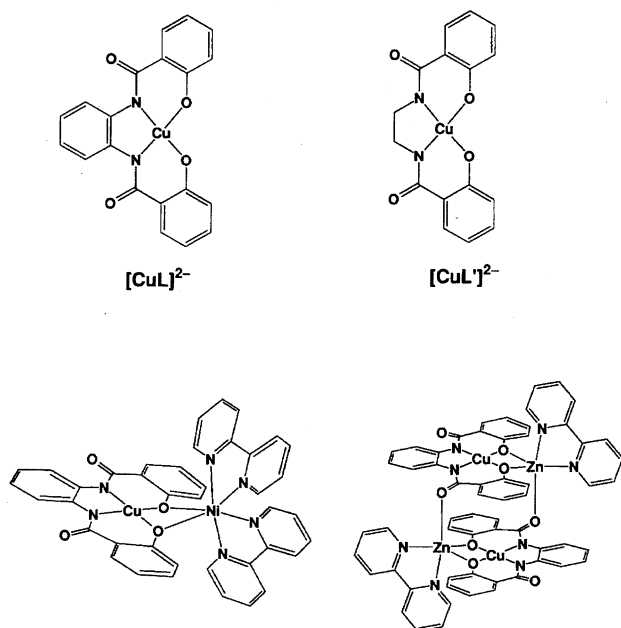
(Received May 25, 1998)

Dipotassium *N,N'*-1,2-phenylenebis(2-carbamoyl-*N*-phenolato-*N*O)cuprate(II), K₂[CuL], reacts with nickel(II), cobalt(II), and zinc(II) acetates, and 2,2'-bipyridine in a 1:1:2 molar ratio in methanol to yield the hetero-metal dinuclear complexes [CuLNi(bpy)₂]₂·3MeOH (**1**·3MeOH), [CuLCo(bpy)₂]₂·2DMF (**2**·2DMF), and [CuLZn(bpy)₂]₂·1.5H₂O (**3**), respectively. Crystal data for **1**: *P* $\bar{1}$ (No. 2) with *a* = 15.969(2), *b* = 23.494(3), *c* = 12.705(2) Å, α = 92.15(1), β = 91.652(10), γ = 101.521(9)°, *V* = 4663(1) Å³, and *Z* = 4; **2**, *P*2₁/*c* (No. 14) with *a* = 12.604(3), *b* = 24.364(5), *c* = 13.823(2) Å, β = 94.49(1)°, *V* = 4231(1) Å³, and *Z* = 4. **1** and **2** have a similar discrete di- μ -phenoxo-bridged dinuclear structure, in which the Cu(II) ion assumes a square-planar geometry with the N₂O₂ donors atoms consisting of two amido nitrogen and two phenoxo oxygen atoms of the tetradentate ligand, and the Ni(II) or Co(II) ion assumes an octahedral geometry with the two phenoxo oxygens of the tetradentate ligand and four nitrogen atoms from two bpy. The magnetic-susceptibility data were reproduced based on the isotropic spin Hamiltonian $\mathbf{H} = -2J\mathbf{S}_1 \cdot \mathbf{S}_2$ with *J* = -118.0 cm⁻¹, (*S*₁, *S*₂) = (1/2, 1) for **1** and *J* = -11.0 cm⁻¹, (*S*₁, *S*₂) = (1/2, 3/2) for **2**, respectively. When **3** was recrystallized from DMF/2-propanol, [CuLZn(bpy)₂]₂·2DMF (**3'**) was obtained. The 1:1:1 reaction of K₂[CuL'], copper(II) acetate monohydrate, and 2,2'-bipyridine in methanol yielded [CuL'Cu(bpy)₂]₂·2MeOH (**4**), (H₄L' = 1,2-bis(hydroxybenzamido)ethane). Crystal data for **3'**: *Pbca* (No. 61) with *a* = 19.143(2), *b* = 18.195(2), *c* = 16.832(3) Å, and *Z* = 4; **4**, *P*2₁/*n* (No. 14) with *a* = 13.407(1), *b* = 13.172(4), *c* = 13.764(2) Å, β = 94.11(1)°, *V* = 2424.4(8) Å³, and *Z* = 4. **3'** and **4** have a similar cyclic di- μ -phenoxo- μ -amido-bridged tetranuclear structure, which can be described as two di- μ -phenoxo-bridged dinuclear units bridged together by the coordination of one amido oxygen atom from each dinuclear unit to the zinc(II) or copper(II) ion of the other dinuclear unit, with Zn(1)-O(3)* = 2.004(3) and Cu(2)-O(4)* = 1.924(4) Å bond distances, respectively. In the tetranuclear structure, the copper(II) ion coordinated by the tetradentate ligand assumes a square-planar geometry and the zinc(II) or the other copper(II) ion assumes a square-pyramidal coordination geometry with two phenoxo-oxygen atoms, two nitrogen atoms of bpy, and one amido oxygen atom. The magnetic susceptibility of **4** was reproduced by an equation derived from the $\mathbf{H} = -2J(\mathbf{S}_1 \cdot \mathbf{S}_2 + \mathbf{S}_3 \cdot \mathbf{S}_4) - 2J'(\mathbf{S}_2 \cdot \mathbf{S}_3 + \mathbf{S}_4 \cdot \mathbf{S}_1)$ spin Hamiltonian with *J* = -14.6 cm⁻¹ and *J'* = -4.0 cm⁻¹.

Multinuclear hetero-metal complexes are of great interest not only in elucidating the magnetic coupling between different metal ions and developing complex-based magnetic materials,¹⁾ but also in model compounds of the active site of multinuclear metalloenzymes.²⁾ The hetero-metal polynuclear complexes are still limited by the small number of known and fully characterized compounds and by the relative difficulty of synthesizing such new compounds. Two synthetic strategies have been developed for the synthesis of hetero-metal complexes. One of them uses a polynucleating ligand providing nonequivalent coordination environments for different metal ions.³⁾ The other one uses a "ligand-complex"

exhibiting coordination ability to metal ions.⁴⁾ The "ligand-complex" method is effective for the synthesis of hetero-metal polynuclear complexes with a systematic combination of metal ions. For example, the copper(II) complex resulting from a 1:1:1 condensation of 4-formylimidazole, ethylenediamine, and acetylacetone is a typical "ligand-complex", and the imidazolate nitrogen atom of its deprotonated form acts as a monodentate ligand towards other metal ions to yield a series of imidazolate-bridged hetero-metal complexes.⁵⁾

In order to synthesize a new type of hetero-metal complexes and furthermore to obtain extended multi-dimensional structures, new multidentate ligand-complexes should



Scheme 1.

be developed. From this viewpoint, *N,N'*-trimethylenebis-(oxamato- $\kappa N, \kappa O$)cuprate(II) is a representative multidentate ligand complex in which the two oxamato groups, functioning as a bidentate ligand, are oriented to opposite directions in a line. By using the ligand-complex, Kahn et al. have synthesized a linear one-dimensional Mn(II)–Cu(II) complex showing spontaneous magnetic ordering.⁶ In order to improve the dimensionality from extended one- to two- or three-dimensional structures, they have used 2,2'-(*N,N'*-oxamidato- $\kappa^2 N$)bis(benzoato- κO)cuprate(II), because the orientation of the donor atoms of this complex is bent from a line. The reaction of the ligand-complex with Mn(II) ions gave a ferromagnet with high critical temperature.⁷

In order to synthesize new hetero-metal polynuclear complexes and to develop metal-complex based magnetic materials along this line, we have focused our effort on copper(II) and other metal complexes with 1,2-bis(2-hydroxybenzamido)benzene (H_4L) and 1,2-bis(2-hydroxybenzamido)ethane (H_4L')⁸ because their complexes can act as multidentate ligands, not only at the two phenoxo oxygen atoms, but also at the two amido oxygen atoms. In this paper, we report on the syntheses, characterization, magnetic properties, and crystal structures of di- μ -phenoxo-bridged hetero-metal dinuclear Cu(II)–Ni(II) and Cu(II)–Co(II) complexes and cyclic di- μ -phenoxo- μ -amido-bridged tetranuclear Cu_4^{II} and Cu_2^{II} – Zn_2^{II} complexes (Scheme 1), which were prepared by a reaction of the ligand-complex with the second metal ion and 2,2'-bipyridine as the terminal capping ligand.

Experimental

Materials. All reagents and solvents used in this study are commercially available and were used without further purification. The solvent used for physical measurements were purified by literature methods⁹ and stored under nitrogen.

Synthesis. 1,2-bis(2-hydroxybenzamido)benzene (H_4L) was

prepared according to a literature method.¹⁰ The Cu(II) precursor complex, $K_2[CuL] \cdot 1.5H_2O$, was prepared according to a previously reported method.^{8a)}

[CuLNi(bpy)₂] \cdot 1.5H₂O (1 \cdot 1.5H₂O). $K_2[CuL] \cdot 1.5H_2O$ (0.513 g, 1 mmol) and nickel(II) acetate tetrahydrate (0.249 g, 1 mmol) were mixed in methanol (40 mL) and stirred for 1 h. To this solution was added 2,2'-bipyridine (0.312 g, 2 mmol) in methanol (10 mL), and the resulting solution was further stirred for 1 h. The olive-green microcrystals which precipitated upon standing were suction-filtered, washed with methanol and dried in vacuo. Anal. Calcd for $C_{40}H_{31}N_6O_{5.5}NiCu$: C, 59.61; H, 3.87; N, 10.42%. Found: C, 59.44; H, 3.78; N, 10.25%. IR 1597 cm^{-1} (ν_{CO} (amido)). UV ($\log \epsilon$) 567 nm (1.87) in DMSO. μ_{eff} (300 K)/CuNi, 3.71 μ_B .

[CuLNi(bpy)₂] \cdot 3MeOH (1 \cdot 3MeOH). Single crystals suitable for X-ray crystallographic studies were prepared as follows. $K_2[CuL] \cdot 1.5H_2O$ (0.257 g, 0.5 mmol) and nickel(II) acetate tetrahydrate (0.125 g, 0.5 mmol) were mixed in methanol (40 mL). 2,2'-Bipyridine (0.156 g, 1 mmol) in methanol (10 mL) was added to the mixture and the solution was left standing for 1 week, yielding dark reddish-brown crystals. The infrared spectra of 1 \cdot 1.5H₂O and 1 \cdot 3MeOH are identical, except for those of the solvent molecules.

[CuLCo(bpy)₂] \cdot 1.5H₂O (2 \cdot 1.5H₂O). This complex was prepared similarly to 1 using cobalt(II) acetate tetrahydrate instead of nickel(II) acetate tetrahydrate. Dark yellowish-brown microcrystals were obtained. Anal. Calcd for $C_{40}H_{29}N_6O_{4.5}CoCu$: C, 59.59; H, 3.86; N, 10.42%. Found: C, 59.88; H, 3.75; N, 10.42%. IR 1600 cm^{-1} (ν_{CO} (amido)). UV ($\log \epsilon$) 539 nm (1.85) in DMSO. μ_{eff} (300 K)/CuCo, 5.09 μ_B .

[CuLCo(bpy)₂] \cdot 2DMF (2 \cdot 2DMF). Single crystals suitable for X-ray analyses were prepared by recrystallization from a DMF/2-propanol solvent mixture: Highly efflorescent yellowish-brown crystals with the $[CuLCo(bpy)_2] \cdot 2DMF$ formula were thus obtained. The infrared spectra of 2 \cdot 1.5H₂O and 2 \cdot 2DMF are identical, except for those of the solvent molecules.

[CuLZn(bpy)₂] \cdot 1.5H₂O (3). This complex was prepared similarly to 1 by using zinc(II) acetate dihydrate instead of nickel(II) acetate tetrahydrate. Dark-green microcrystals were obtained. Anal. Calcd for $C_{30}H_{31}N_5O_{5.5}CuZn$: C, 59.12; H, 3.84; N, 10.34%. Found: C, 59.12; H, 3.71; N, 10.26%. IR 1594 cm^{-1} (ν_{CO} (amido)). UV ($\log \epsilon$) 580 nm (1.74) in DMSO. μ_{eff} (300 K) per CuZn, 1.84 μ_B .

[CuLZn(bpy)₂] \cdot 2DMF (3'). This compound was obtained by recrystallizing $[CuLZn(bpy)_2] \cdot 1.5H_2O$ from DMF/2-propanol. A DMF solution of 3 was diffused to 2-propanol at room temperature. After standing for several days, black crystals were obtained. Anal. Calcd for $C_{66}H_{54}N_{10}O_{10}Cu_2Zn_2$: C, 56.42; H, 3.87; N, 9.97%. Found: C, 56.28; H, 4.12; N, 9.97%. IR 1672 cm^{-1} (ν_{CO} (DMF)), 1600 cm^{-1} (ν_{CO} (amido)). UV ($\log \epsilon$) 580 nm (1.74) in DMSO. μ_{eff} (300 K) per CuZn, 1.76 μ_B .

[CuL'Cu(bpy)₂] \cdot 2MeOH (4). This compound was prepared by a 1 : 1 : 1 reaction of $K_2[CuL']$, copper(II) acetate monohydrate, and 2,2'-bipyridine in methanol ($H_4L' = 1,2$ -bis(2-hydroxybenzamido)ethane) according to the previously reported method.⁸ The microcrystalline product was recrystallized from a DMF/MeOH solvent mixture to yield dark-red prismatic crystals suitable for X-ray analysis. Anal. Calcd for $C_{54}H_{48}N_8O_{10}Cu_4$: C, 53.02; H, 3.96; N, 9.16%. Found: C, 52.93; H, 3.94; N, 8.86%. IR 1597 cm^{-1} (ν_{CO} (amido)). UV ($\log \epsilon$) 567 nm (1.87) in DMSO. μ_{eff} (300 K) per Cu, 1.58 μ_B .

Physical Measurements. Elemental analyses for C, H, and N were carried out at the Elemental Analysis Service Center of Kyushu University. Metal analyses were performed on a Hitachi

508 atomic-absorption spectrophotometer. Infrared spectra were recorded on a JASCO A-102 spectrophotometer using KBr disks. Electronic spectra were measured on a Hitachi U-4000 spectrophotometer using 1 cm quartz cells and ca. 10^{-3} mol dm $^{-3}$ solution. Electrical conductivities were measured on a Horiba conductivity meter (DS-14) in ca. 10^{-3} mol dm $^{-3}$ solution. Electrochemical measurements were carried out on a Yanagimoto P-1100 polarographic analyzer equipped with a glassy carbon working electrode, a platinum wire auxiliary electrode and a saturated calomel electrode (SCE) as the reference. Tetrabutylammonium perchlorate (TBAP, ca. 10^{-1} mol dm $^{-3}$) was employed as the supporting electrolyte. Alkali metal cations were added as perchlorate salts. X-band ESR spectra were recorded with a JEOL TE 200 spectrometer on a frozen DMF solution and powder samples at liquid-nitrogen temperature. The magnetic susceptibilities were measured with a MPMS SQUID susceptometer (Quantum Design Inc.) in the 2–300 K temperature range under a 1 T. Diamagnetic corrections were applied by using Pascal's constants.¹¹ Effective magnetic moments were calculated by the equation $\mu_{\text{eff}} = 2.828(\chi_{\text{M}} \times T)^{1/2}$, where χ_{M} is the molar magnetic susceptibility. Fitting of the magnetic data to the theoretical expressions was performed with a commercially available software (Kaleida Graph).

X-Ray Crystal Structure Analysis. The single crystals of [CuLZn(bpy)] $_2$ ·2DMF (**3'**) and [CuL'/Cu(bpy)] $_2$ ·2MeOH (**4**) are stable in the air and the crystals were mounted on a glass rod. Since the crystals of [CuLNi(bpy)] $_2$ ·3MeOH (**1**·3MeOH) and [CuLCo(bpy)] $_2$ ·2DMF (**2**·2DMF) decompose easily due to the evaporation of the crystal solvents, each crystal was encapsulated into a glass capillary with a small amount of mother liquor. All crystallographic measurements were carried out on a Rigaku AFC7R diffractometer with graphite monochromated MoK α radiation ($\lambda = 0.71069$ Å) and a 12 kW rotating anode generator. The data were collected at a temperature of $20 \pm 1^\circ\text{C}$ using the ω - 2θ scan mode at a $16.0^\circ \text{min}^{-1}$ scan speed. The intensities of three representative reflections were measured after every 150 reflections, showing a good stability of the intensities. An empirical absorption correction based on azimuthal scans of several reflections was applied. The

data were corrected for Lorentz and polarization effects.

The structures were solved by direct methods and expanded using Fourier techniques.¹² The non-hydrogen atoms were refined anisotropically. Hydrogen atoms at the calculated ideal positions were included in the structure-factor calculation, but not refined. Full-matrix least-squares refinement based on the observed reflections ($I > 3\sigma(I)$) were employed, with unweighted and weighted agreement factors $R = \sum ||F_o| - |F_c|| / \sum |F_o|$ and $R_w = [\sum w(|F_o| - |F_c|)^2 / \sum w|F_o|^2]^{1/2}$. The weighting scheme was based on counting statistics. Neutral atomic-scattering factors were taken from Cromer and Waber.¹³ Anomalous dispersion effects were included in F_{calc} ; the values $\Delta f'$ and $\Delta f''$ were those of Creagh and McAuley.¹⁴ All of the calculations were performed using the teXsan crystallographic software package of Molecular Structure Corporation.¹⁵ Crystal data are summarized in Table 1. Tables of the crystal data, atom coordinates, complete bond distances and angles, anisotropic displacement factors, and calculated hydrogen coordinates (69 pages) and $F_o - F_c$ data are deposited as Document No. 71054 at the Office of the Editor of Bull. Chem. Soc. Jpn.

Results and Discussion

Synthesis and Characterization. The K $_2$ [CuL] ligand-complex reacts with Ni(II), Co(II), and Zn(II) acetate, and 2, 2'-bipyridine (bpy) as the capping ligand, in a 1 : 1 : 2 molar ratio in methanol to yield the electrically neutral hetero-metal dinuclear complexes [CuLNi(bpy)] $_2$ (**1**), [CuLCo(bpy)] $_2$ (**2**), and [CuLZn(bpy)] $_2$ (**3**), respectively. When **3** was recrystallized from DMF/2-propanol, [CuLZn(bpy)] $_2$ ·2DMF (**3'**·2DMF) was obtained. The 1 : 1 : 1 reaction of K $_2$ [CuL'], Cu(II) acetate monohydrate as the second metal ion, and bpy as the terminal capping ligand in methanol yield [CuL'/Cu(bpy)] $_2$ ·2MeOH (**4**·2MeOH).

Structural Description of [CuLNi(bpy)] $_2$ ·3MeOH (1**·3MeOH).** Although the crystal consists of two crystallographically independent dinuclear molecules, the two

Table 1. Crystallographic Data for [CuLNi(bpy)] $_2$ ·3MeOH (**1**·3MeOH), [CuLCo(bpy)] $_2$ ·2DMF (**2**·2DMF), [CuLZn(bpy)] $_2$ ·2DMF (**3'**), and [CuL'/Cu(bpy)] $_2$ ·2MeOH (**4**)

	[CuLNi(bpy)] $_2$ ·3MeOH	[CuLCo(bpy)] $_2$ ·2DMF	[CuLZn(bpy)] $_2$ ·2DMF	[CuL'/Cu(bpy)] $_2$ ·2MeOH
Formula	C $_43$ H $_40$ N $_6$ O $_7$ NiCu	C $_46$ H $_42$ N $_8$ O $_6$ CoCu	C $_66$ H $_54$ N $_{10}$ O $_{10}$ Cu $_2$ Zn $_2$	C $_54$ H $_48$ N $_8$ O $_{10}$ Cu $_4$
Formula weight	875.07	925.37	1405.07	1223.20
Crystal color	Reddish brown	Light yellowish brown	Black	Dark red
Crystal system	Triclinic	Monoclinic	Orthorhombic	Monoclinic
Space group	$P\bar{1}$ (No. 2)	$P2_1/c$ (No. 14)	$Pbca$ (No. 61)	$P2_1/n$ (No. 14)
$a/\text{Å}$	15.969(2)	12.604(3)	19.143(2)	13.407(1)
$b/\text{Å}$	23.494(3)	24.364(5)	18.195(2)	13.172(4)
$c/\text{Å}$	12.705(2)	13.823(2)	16.832(3)	13.764(2)
α/deg	92.15(1)	90	90	90
β/deg	91.652(10)	94.49(1)	90	94.108(10)
γ/deg	101.521(9)	90	90	90
$V/\text{Å}^3$	4663(1)	4231(1)	5862(1)	2424.4(8)
Z	4	4	4	4
$D_{\text{calc}}/\text{g cm}^{-3}$	1.246	1.452	1.592	1.675
μ/cm^{-1}	9.10	9.55	15.96	18.03
No. of Reflections	17057	8933	6372	4690
R	0.074	0.052	0.039	0.042
R_w	0.088	0.044	0.030	0.038

$$R = \sum ||F_o| - |F_c|| / \sum |F_o|, R_w = [\sum w(|F_o| - |F_c|)^2 / \sum w|F_o|^2]^{1/2}, w = 1/[\sigma(F_o)^2].$$

molecules are essentially the same, both in geometry and dimensions. Thus, an ORTEP view of only one of the two dinuclear units is shown in Fig. 1. Selected bond distances and angles are given in Table 2.

The X-ray analysis confirmed a discrete di- μ -phenoxo-bridged dinuclear Cu(II)–Ni(II) structure with Cu \cdots Ni distances of 3.025(2) and 3.043(2) Å for the different dinuclear molecules in the asymmetric unit. The dihedral angles between the Cu(II) and Ni(II) coordination planes defined by CuN₂O₂ and NiO₂N₂ are 141.6° and 152.3° for the two different dinuclear molecules in the asymmetric unit, showing a substantial bending between the equatorial coordination planes and non-planarity of the CuNiO₂ core. In the dinuclear structure, the copper(II) ion assumes a square-planar coordination geometry with the N₂O₂ donor sets consisting of two amido nitrogen and two phenoxo oxygen atoms of the tetradentate ligand. The average distances for the Cu–N and Cu–O bonds are 1.91 and 1.927 Å, respectively, which can be compared to the corresponding values in the precursor mononuclear complex, K₂[CuL]·5DMF, (Cu–N = 1.938 Å and Cu–O = 1.917 Å).^{8c} The Cu–O distance in the present dinuclear compound is slightly longer than that in the precursor complex due to the formation of a phenoxo bridge, while, on the contrary, the Cu–N distance is slightly shorter than that in the precursor complex. In the dinuclear structure, the nickel(II) ion assumes a distorted octahedral geometry with the N₄O₂ donor set arising from two phenoxo oxygen atoms, and four nitrogen atoms of two bpy molecules, with average Ni–N = 2.09 Å and Ni–O = 2.109 Å bond distances.

Structural Description of [CuLCo(bpy)₂]-2DMF (2·2DMF). An ORTEP view of the molecule with atom numbering is shown in Fig. 2 and selected bond distance and angles are given in Table 3.

The crystal consists of a di- μ -phenoxo-bridged dinuclear Cu(II)–Co(II) molecule with a Cu \cdots Co distance of 3.072(1) Å and two DMF molecules as the crystal solvent. The over-

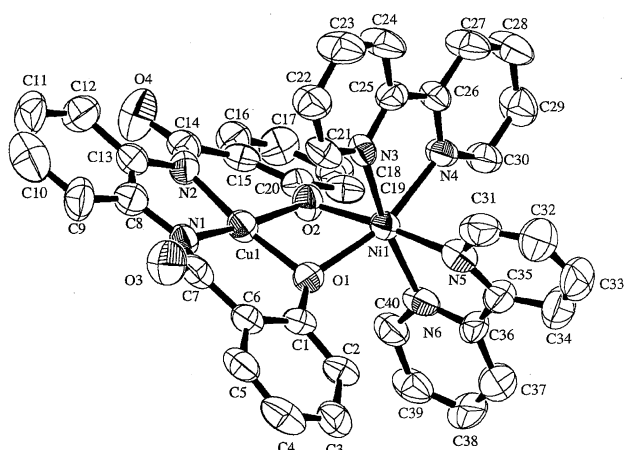


Fig. 1. An ORTEP drawing of [CuLNi(bpy)₂]-3MeOH (1·3MeOH) with atom numbering, showing 50% probability ellipsoids. The crystal consists of two crystallographically independent dinuclear molecules. As the two molecules are essentially the same, only one of them is shown.

Table 2. Selected Bond Distances (Å) and Angles (deg) for [CuLNi(bpy)₂]-3MeOH (1·3MeOH)

Bond distances			
Cu(1)–O(1)	1.928(8)	Cu(1)–O(2)	1.920(8)
Cu(1)–N(1)	1.94(1)	Cu(1)–N(2)	1.89(1)
Ni(1)–O(1)	2.068(8)	Ni(1)–O(2)	2.142(8)
Ni(1)–N(3)	2.064(9)	Ni(1)–N(4)	2.074(9)
Ni(1)–N(5)	2.09(1)	Ni(1)–N(6)	2.09(1)
Cu(2)–O(5)	1.925(7)	Cu(2)–O(6)	1.933(8)
Cu(2)–N(7)	1.90(1)	Cu(2)–N(8)	1.91(1)
Ni(2)–O(5)	2.091(8)	Ni(2)–O(6)	2.136(8)
Ni(2)–N(9)	2.12(1)	Ni(2)–N(10)	2.11(1)
Ni(2)–N(11)	2.10(1)	Ni(2)–N(12)	2.08(1)
Cu(1)–Ni(1)	3.025(2)	Cu(2)–Ni(2)	3.043(2)
Bond angles			
O(1)–Cu(1)–O(2)	82.0(3)	N(1)–Cu(1)–N(2)	87.9(5)
O(1)–Cu(1)–N(1)	95.8(4)	O(2)–Cu(1)–N(2)	93.5(4)
O(1)–Ni(1)–O(2)	73.6(3)	N(4)–Ni(1)–N(5)	89.6(4)
O(1)–Ni(1)–N(5)	103.8(4)	O(2)–Ni(1)–N(4)	93.8(4)
N(3)–Ni(1)–N(4)	78.2(4)	N(5)–Ni(1)–N(6)	77.2(5)
N(3)–Ni(1)–N(6)	170.1(4)		
O(5)–Cu(2)–O(6)	83.5(3)	N(7)–Cu(2)–N(8)	86.1(5)
O(5)–Cu(2)–N(7)	95.8(4)	O(6)–Cu(2)–N(8)	94.8(4)
O(5)–Ni(2)–O(6)	74.9(3)	N(10)–Ni(2)–N(11)	88.9(4)
O(5)–Ni(2)–N(11)	105.2(3)	O(6)–Ni(2)–N(10)	92.5(4)
N(9)–Ni(2)–N(10)	77.6(5)	N(11)–Ni(2)–N(12)	78.8(4)
N(9)–Ni(2)–N(12)	176.4(4)		
Cu(1)–O(1)–Ni(1)	98.3(4)	Cu(1)–O(2)–Ni(1)	96.1(4)
Cu(2)–O(5)–Ni(2)	98.4(3)	Cu(2)–O(6)–Ni(2)	96.7(4)

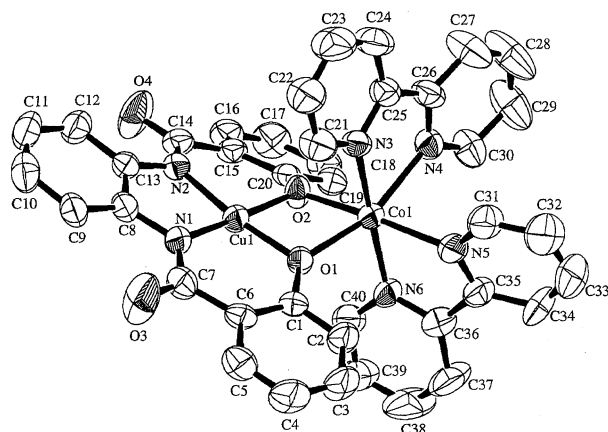


Fig. 2. An ORTEP drawing of [CuLCo(bpy)₂]-2DMF (2·2DMF) with atom numbering, showing 50% probability ellipsoids.

all dinuclear structure is similar to that of 1·3MeOH. The dihedral angle between the CuN₂O₂ and CoN₂O₂ coordination planes is 154.4°. The copper(II) ion assumes a square-planar coordination geometry with average Cu–N = 1.910 Å and Cu–O = 1.921 Å bond distances. The coordination geometry around the cobalt(II) ion is a distorted octahedron with two phenoxo oxygen atoms and four nitrogen atoms from two bpy molecules. The average bond distances are Co–N = 2.149 Å and Co–O = 2.076 Å. The Co–N distance is longer than the Ni–N one in 1·3MeOH, and the Co–O

Table 3. Selected Bond Distance (Å) and Angles (deg) for [CuLCo(bpy)₂]₂·2DMF (2·2DMF)

Bond distances			
Cu(1)–O(1)	1.921(4)	Cu(1)–O(2)	1.920(4)
Cu(1)–N(1)	1.899(5)	Cu(1)–N(2)	1.920(5)
Co(1)–O(1)	2.092(4)	Co(1)–O(2)	2.059(4)
Co(1)–N(3)	2.148(5)	Co(1)–N(4)	2.175(5)
Co(1)–N(5)	2.152(5)	Co(1)–N(6)	2.120(6)
O(3)–C(7)	1.238(8)	O(4)–C(14)	1.249(7)
N(1)–C(7)	1.345(8)	N(2)–C(14)	1.341(8)
Cu(1)–Co(1)	3.072(1)		
Bond angles			
O(1)–Cu(1)–O(2)	81.3(2)	N(1)–Cu(1)–N(2)	87.3(2)
O(1)–Cu(1)–N(1)	96.3(2)	O(2)–Cu(1)–N(2)	94.6(2)
O(1)–Cu(1)–N(2)	172.8(2)	O(2)–Cu(1)–N(1)	174.3(2)
O(1)–Co(1)–O(2)	74.1(2)	N(4)–Co(1)–N(5)	82.3(2)
O(1)–Co(1)–N(5)	109.0(2)	O(2)–Co(1)–N(4)	97.1(2)
N(3)–Co(1)–N(4)	75.7(2)	N(5)–Co(1)–N(6)	77.0(2)
N(3)–Co(1)–N(6)	172.7(2)		
Cu(1)–O(1)–Co(1)	99.8(2)	Cu(1)–O(2)–Co(1)	101.0(2)

distance is slightly shorter than the Ni–O one. The bond distances in the two amido moieties are O(3)–C(7) = 1.238(8) Å, N(1)–C(7) = 1.345(8) Å and O(4)–C(14) = 1.249(7) Å, N(2)–C(14) = 1.341(8) Å, respectively, indicating that the two amido groups are essentially equivalent to each other.

Structural Description of [CuLZn(bpy)]₂·2DMF (3'). An ORTEP view of the cyclic tetranuclear structure of [CuLZn(bpy)]₂ with atom numbering is shown in Fig. 3. Selected bond distances and angles are given in Table 4.

The tetranuclear moiety has an inversion center at the center of the molecule. It can be described as two di- μ -phenoxo-bridged dinuclear [CuZn] units, bridged together by the coordination of one amido oxygen atom of each dinuclear unit to the zinc(II) ion of the associated dinuclear unit with a Zn(1)–O(3)* = 2.005(3) Å bond length. In the tetranuclear structure, the copper(II) ion assumes a square-planar coordination geometry with two amido nitrogen atoms and two phenoxo oxygen atoms, while the zinc(II) ion assumes a penta-coordinated geometry with two phenoxo oxygen atoms, two nitrogen atoms of a bpy molecule, and one amido oxygen of the adjacent dinuclear unit. Addison et al. have introduced the structural index parameter, $\tau = (\beta - \alpha)/60$, for five-coordination geometry, where α and β represent two basal angles ($\beta > \alpha$).¹⁶⁾ For an ideal square pyramid, τ is equal to zero, while it is equal to 1 for an ideal trigonal bipyramid. The 0.46 τ value demonstrates that Zn(1) assumes a distorted square-pyramidal geometry with coordination bond distances of Zn(1)–O(1) = 2.062(3) and Zn(1)–O(2) = 2.001(3) Å in the phenoxo moiety, Zn(1)–O(3)* = 2.005(3) Å in the amido moiety, and Zn(1)–N(3) = 2.111(3) and Zn(1)–N(4) = 2.121(3) Å in the bpy moiety. The bond distances in the non-bridging amido group are O(4)–C(14) = 1.238(5) and N(2)–C(14) = 1.353(5) Å, which are close to the corresponding values for 2·2DMF. On the other hand, the bond distance of the bridging amido group are O(3)–C(7) = 1.289(4) and N(1)–C(7) = 1.327(5) Å. The

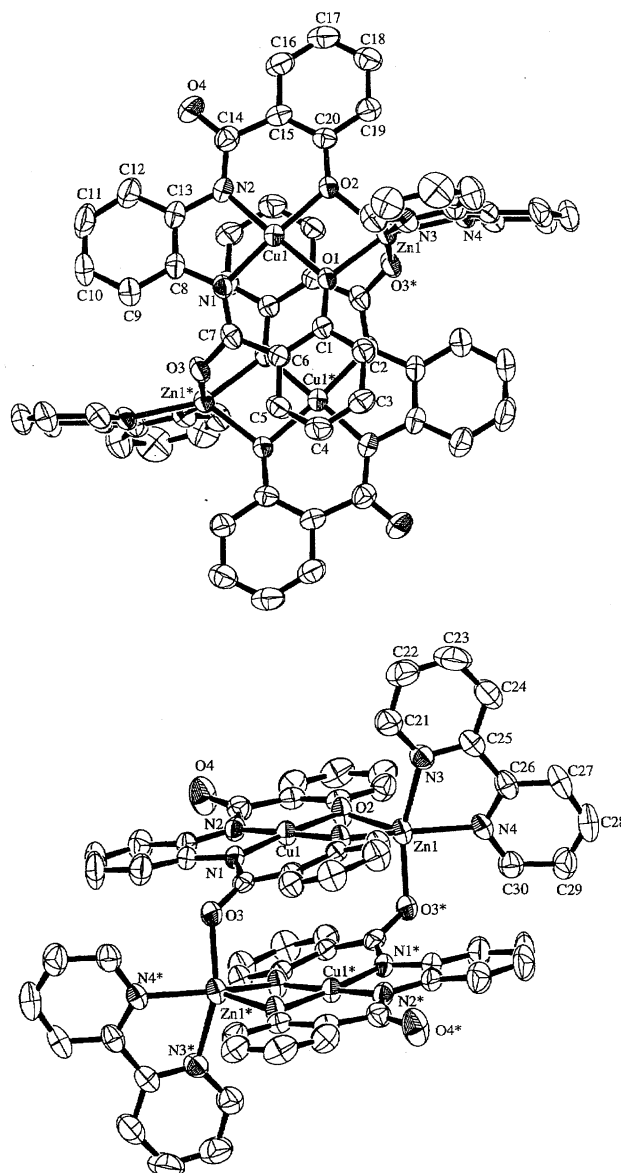


Fig. 3. ORTEP drawings of [CuLZn(bpy)]₂·2DMF (3') with the atom numbering of the asymmetric unit, showing 50% probability ellipsoids. (top) projection on the molecular plane of [CuL]. (bottom) side view.

O–C distance is 0.05 Å longer and the N–C distance is 0.03 Å shorter than those of the corresponding non-bridging amido group, indicating that the O=C double-bond character is weakened due to bridging of the amido group.

Structural Description of [CuL'Cu(bpy)]₂·2MeOH (4). An ORTEP view of the cyclic tetranuclear structure of [CuL'Cu(bpy)]₂ with atom numbering is shown in Fig. 4. Selected bond distances and angles are given in Table 5.

The structure is similar to that of 3'. The Cu(1) atom assumes a square-planar coordination geometry with two amido nitrogen atoms and two phenoxo oxygen atoms of the tetradentate ligand. Cu(2) assumes a five-coordinated distorted square-pyramidal geometry, in which the equatorial sites are occupied by O(2), O(4)*, N(3), and N(4), and the apical site is occupied by O(1). The structural index pa-

Table 4. Selected Bond Distances (Å) and Angles (deg) for [CuLZn(bpy)]₂·2DMF (3')

Bond distances			
Zn(1)–O(1)	2.062(3)	Zn(1)–O(2)	2.001(3)
Zn(1)–O(3)*	2.005(3)		
Zn(1)–N(3)	2.111(3)	Zn(1)–N(4)	2.121(3)
Cu(1)–O(1)	1.913(3)	Cu(1)–O(2)	1.935(3)
Cu(1)–N(1)	1.933(3)	Cu(1)–N(2)	1.904(3)
O(3)–C(7)	1.289(4)	O(4)–C(14)	1.238(5)
N(1)–C(7)	1.327(5)	N(2)–C(14)	1.353(5)
Zn(1)–Zn(1)*	6.931(1)	Cu(1)–Cu(1)*	5.020(1)
Zn(1)–Cu(1)	3.0336(7)		
Bond angles			
O(1)–Zn(1)–O(2)	76.3(1)	O(1)–Zn(1)–O(3)*	91.3(1)
O(1)–Zn(1)–N(3)	93.6(1)	O(1)–Zn(1)–N(4)	153.5(1)
O(2)–Zn(1)–O(3)*	104.5(1)	N(3)–Zn(1)–N(4)	76.9(1)
O(2)–Zn(1)–N(3)	98.4(1)	O(2)–Zn(1)–N(4)	129.2(1)
O(3)*–Zn(1)–N(3)	157.0(1)	O(3)*–Zn(1)–N(4)	88.8(1)
O(1)–Cu(1)–O(2)	81.4(1)	N(1)–Cu(1)–N(2)	87.2(1)
O(1)–Cu(1)–N(1)	95.0(1)	O(2)–Cu(1)–N(2)	96.3(1)
Zn(1)–O(1)–Cu(1)	99.4(1)	Zn(1)–O(2)–Cu(1)	100.8(1)

parameter of Cu(2) is $\tau = 0.58$. The coordination geometry of Cu(2) in **4** is thus more distorted towards a trigonal bipyramid than that of Zn(1) in **3'**. The bond distances in the free amido group are O(3)–C(7) = 1.275(7) and N(1)–C(7) = 1.311(8) Å and the corresponding distances in the bridging amido group are O(4)–C(10) = 1.294(7) and N(2)–C(10) = 1.301(8) Å, showing the same trend in **3'**.

The tetranuclear structures of **3'** and **4** demonstrate that the copper(II) complexes with the H₄L and H₄L' ligands can function as multidentate ligands, not only at the two phenoxo oxygen atoms, but also at the amido oxygen atom.

Magnetic Properties. The magnetic behavior of **1**·1.5H₂O and **2**·1.5H₂O is shown in Fig. 5, in the form of μ_{eff} vs. T plots, where the effective magnetic moments per dinuclear molecule are given. The theoretical curves using the best-fit parameters are drawn as the solid lines in Fig. 5.

The 3.15 μ_{B} room-temperature effective magnetic moment for [CuLNi(bpy)]₂·1.5H₂O (**1**·1.5H₂O) corresponds to the spin-only value for a magnetically dilute (S_{Cu} , S_{Ni}) = (1/2, 1) spin-system. Upon lowering the temperature, the magnetic moment decreases from 3.15 μ_{B} at 300 K to 2.04 μ_{B} at 2 K, indicating the operation of antiferromagnetic interactions. This magnetic behavior is reproduced by the magnetic-susceptibility expression (1) based on the $\mathbf{H} = -2JS_{\text{Cu}} \cdot \mathbf{S}_{\text{Ni}}$ isotropic spin-Hamiltonian for a dinuclear Cu(II)–Ni(II) spin system.

$$\chi_{\text{M}} = \frac{N\beta^2}{4kT} [10g_{3/2}^2 + g_{1/2}^2 \exp(-J/kT)] / [2 + \exp(-J/kT)] + N\alpha \quad (1)$$

In Eq. 1, N is Avogadro's number, β is the Bohr magneton, k is the Boltzmann constant, J is the exchange integral, $N\alpha$ is the temperature independent paramagnetism, and $g_{1/2} = (4g_{\text{Ni}} - g_{\text{Cu}})/3$ and $g_{3/2} = (2g_{\text{Ni}} + g_{\text{Cu}})/3$. The best-fit parameters are $J = -118.0 \text{ cm}^{-1}$, $g_{\text{Cu}} = 1.99$, $g_{\text{Ni}} = 2.35$,

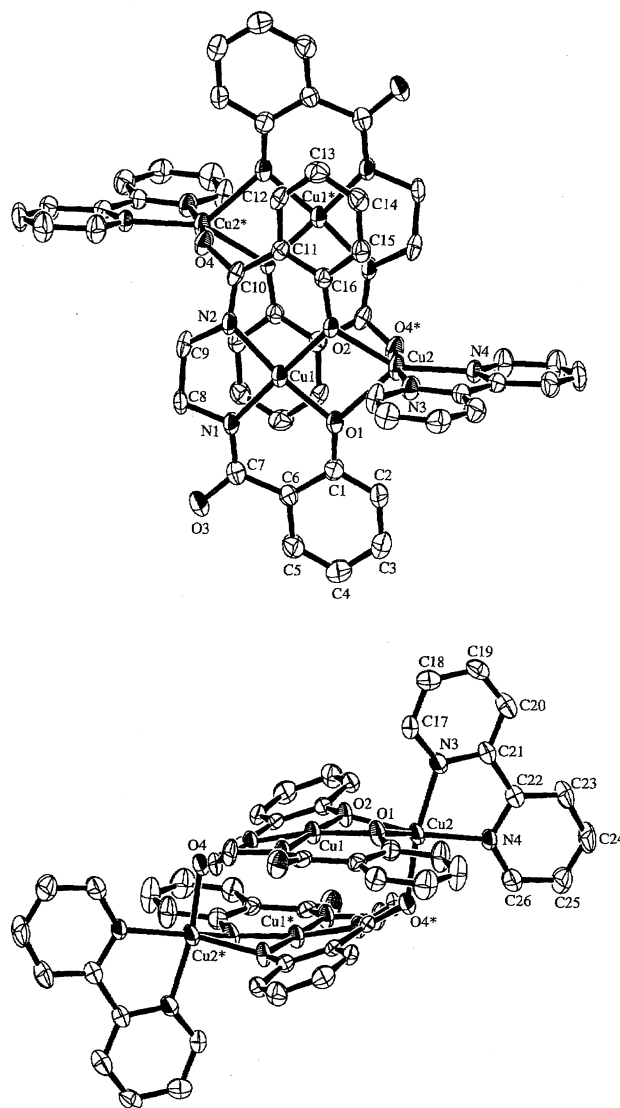


Fig. 4. ORTEP drawings of [CuL'Cu(bpy)]₂·2DMF (**4**) with the atom numbering of the asymmetric unit, showing 50% probability ellipsoids. (top) projection on the molecular plane of [CuL']. (bottom) side view.

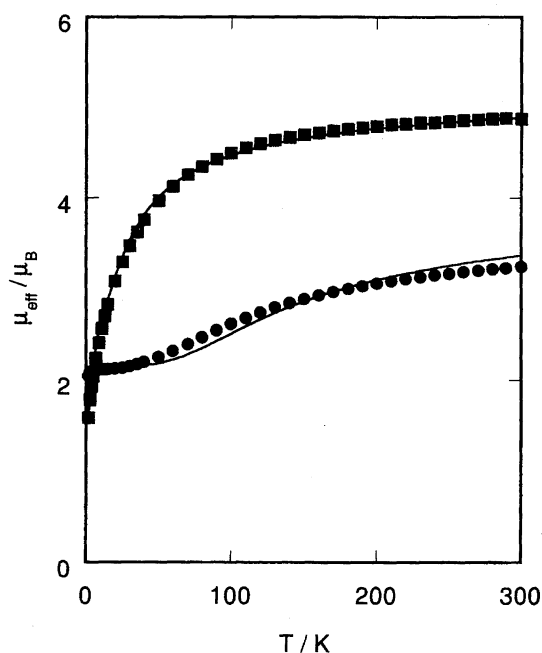
$$N\alpha = 220 \times 10^{-6} \text{ cm}^3 \text{ mol}^{-1}.$$

The 5.09 μ_{B} room-temperature μ_{eff} value for [CuLCo(bpy)]₂·1.5H₂O (**2**·1.5H₂O) corresponds to the spin-only value for the magnetically dilute (S_{Cu} , S_{Co}) = (1/2, 3/2) spin-system. Upon lowering the temperature, the magnetic moment decreases from 5.09 μ_{B} at 300 K to 1.62 μ_{B} at 2 K, indicating the operation of antiferromagnetic interaction. This magnetic behavior is well reproduced by expression (2) based on the $\mathbf{H} = -2JS_{\text{Cu}} \cdot \mathbf{S}_{\text{Co}} + g\beta S_{\text{Z}}H - zJ' < S_{\text{Z}} > \mathbf{S}_{\text{Z}}$ isotropic spin-Hamiltonian for a dinuclear Cu(II)–Co(II) spin system including intermolecular interactions in the molecular-field approximation.¹⁷⁾

$$\chi_{\text{M}} = N\beta^2 g_{\text{(total)}} \{ [10 + 2\exp(-4J/kT)] / [5 + 3\exp(-4J/kT)] \} [kT - zJ' \{ [10 + 2\exp(-4J/kT)] / [5 + 3\exp(-4J/kT)] \}]^{-1} + N\alpha \quad (2),$$

Table 5. Selected Bond Distances (Å) and Angles (deg) for [CuL'Cu(bpy)]₂·2MeOH (4)

Bond distances			
Cu(1)–O(1)	1.911(4)	Cu(1)–O(2)	1.925(4)
Cu(1)–N(1)	1.897(5)	Cu(1)–N(2)	1.921(5)
Cu(2)–O(1)	2.169(4)	Cu(2)–O(2)	2.076(4)
Cu(2)–O(4)*	1.924(4)		
Cu(2)–N(3)	1.991(5)	Cu(2)–N(4)	2.019(5)
O(3)–C(7)	1.275(7)	O(4)–C(10)	1.294(7)
N(1)–C(7)	1.311(8)	N(2)–C(10)	1.301(8)
Cu(1)–Cu(2)	3.097(1)	Cu(1)–Cu(1)*	4.984(2)
Cu(2)–Cu(2)*	5.108(1)		
Bond angles			
O(1)–Cu(1)–O(2)	82.8(2)	N(1)–Cu(1)–N(2)	87.2(2)
O(1)–Cu(1)–N(1)	95.4(2)	O(1)–Cu(1)–N(2)	170.4(2)
O(2)–Cu(1)–N(1)	177.4(2)	O(2)–Cu(1)–N(2)	94.3(2)
O(1)–Cu(2)–O(2)	73.4(2)	N(3)–Cu(2)–N(4)	80.3(2)
O(1)–Cu(2)–O(4)*	95.7(2)	O(2)–Cu(2)–O(4)*	95.0(2)
O(1)–Cu(2)–N(3)	90.4(2)	O(1)–Cu(2)–N(4)	135.1(2)
O(2)–Cu(2)–N(3)	93.9(2)	O(2)–Cu(2)–N(4)	150.4(2)
O(4)–Cu(2)–N(3)	170.4(2)	O(4)–Cu(2)–N(4)	90.1(2)
Cu(1)–O(1)–Cu(2)	98.5(2)	Cu(1)–O(2)–Cu(2)	101.4(2)

Fig. 5. Temperature dependence of the effective magnetic moment for **1**·1.5H₂O (●) and **2**·1.5H₂O (■). The solid lines represent the calculated curves using the best-fit parameters mentioned in the text.

where $g_{\text{total}} = (3g_{\text{Co}} + g_{\text{Cu}})/4$. The best-fit parameters are $J = -7.3 \text{ cm}^{-1}$, $g_{\text{Co}} = 2.32$, $g_{\text{Cu}} = 2.11$, $zJ' = -6.9 \text{ cm}^{-1}$, $N\alpha = 300 \times 10^{-6} \text{ cm}^3 \text{ mol}^{-1}$.

The J value for **1**·1.5H₂O is larger than that for **2**·1.5H₂O, which is the usual trend for hetero-metallic Cu(II)–M(II) dinuclear systems (M = Cu, Ni, Co, Mn), in which the J value decreases as the number of M(II) unpaired electrons increases.¹⁸⁾

The magnetic behaviors of **3'** and **4** are shown in Fig. 6, in

the form of μ_{eff} vs. T and χ_A vs. T plots, where the effective magnetic moments are given per copper(II) ion. The effective magnetic moment for **3'** is practically constant (1.80–1.75 μ_B) over the 2.0–300 K temperature range. This result indicates that there is no detectable magnetic interaction between Cu(II) ions through the diamagnetic Zn(II) coordination sphere.

The 1.58 μ_B room-temperature effective magnetic moment per Cu(II) ion for the tetranuclear copper(II) complex **4** is smaller than the spin-only value for $S = 1/2$. The value of μ_{eff} decreases from 1.58 μ_B at 300 K to 0.25 μ_B at 2 K, indicating the operation of antiferromagnetic interactions. Upon lowering the temperature, the magnetic susceptibility increases to reach a maximum at 30 K, then decreases, and finally increases from 5 K. The increase in the lowest temperature range is due to a mononuclear paramagnetic impurity. The interpretation of this magnetic behavior is based on the $\mathbf{H} = -2J(\mathbf{S}_1 \cdot \mathbf{S}_2 + \mathbf{S}_3 \cdot \mathbf{S}_4) - 2J'(\mathbf{S}_2 \cdot \mathbf{S}_3 + \mathbf{S}_4 \cdot \mathbf{S}_1)$ spin-Hamiltonian for a cyclic tetranuclear structure.¹⁹⁾ The best-fit parameters are $J = -14.6 \text{ cm}^{-1}$, $J' = -4.0 \text{ cm}^{-1}$, and $g = 2.02$ with $N\alpha = 60 \times 10^{-6} \text{ cm}^3 \text{ mol}^{-1}$.

ESR Spectra of 1·1.5H₂O and 3. The ESR spectra of [CuLNi(bpy)₂]·1.5H₂O (**1**·1.5H₂O) and [CuLZn(bpy)₂]·1.5H₂O (**3**) were measured on frozen DMF solutions at liquid nitrogen temperature. The [CuZn] complex **3** shows an axial ESR pattern with $g_{\parallel} = 2.20$, $g_{\perp} = 2.04$ typical of a planar Cu(II) complex with one unpaired electron in the $d_{x^2-y^2}$ orbital. At variance with the ESR spectrum of **3**, the [CuNi] complex **1** shows an axial pattern with $g_{\perp} = 2.18$ and $g_{\parallel} = 2.09$.

Electrochemical Property. Electrochemical measure-

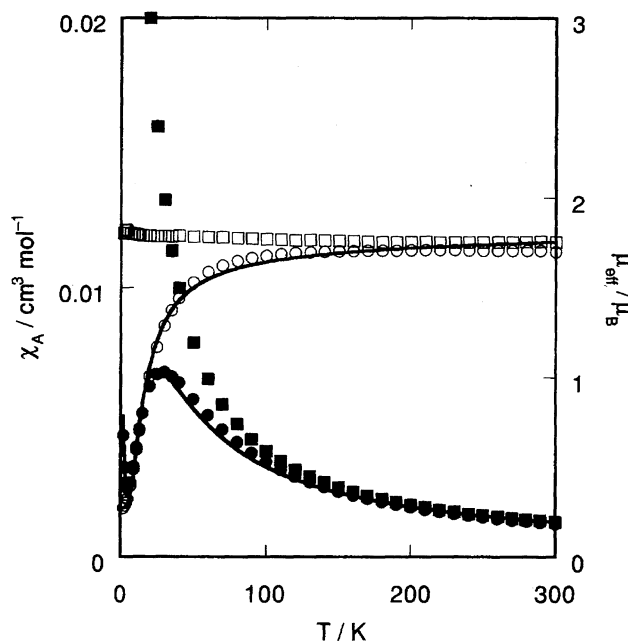
Fig. 6. Temperature dependence of the susceptibilities for **3'** (■) and **4** (●) and the effective magnetic moment for **3'** (□) and **4** (○). The solid lines represent the calculated curves using the best-fit parameters mentioned in the text.

Table 6. Electrochemical Data for the Hetero-metallic Complexes **1**·1.5H₂O, **2**·1.5H₂O, and **3** and the Precursor Complex with their Molar Electrical Conductivities

Complex	$E_{1/2}/V$ Cu(II/III)	$E_{1/2}/V$ M(II/I)	$\Lambda_M/S\text{ cm}^2\text{ mol}^{-1}$
[NMe ₄] ₂ [CuL]·H ₂ O	-0.207 (70)	—	68
[CuLNi(bpy) ₂]·1.5H ₂ O	-0.222	-1.507 (100)	13
[CuLCo(bpy) ₂]·1.5H ₂ O	-0.190 (118)	-1.907 (67)	5
[CuLZn(bpy) ₂]·1.5H ₂ O	-0.144 (86)	—	7

All the observed potentials were given by the difference from the Fc⁺/Fc couple of Ferrocene which was employed as an internal standard. $\Delta E_p/mV$ is given in parenthesis. Tetrabutylammonium perchlorate was employed as supporting electrolyte. All measurements were carried out in DMSO.

ments for the [CuLM(bpy)₂] series (M = Ni (**1**·1.5H₂O), Co (**2**·1.5H₂O), Zn (**3**)) were carried out in DMSO solutions and the potentials, together with the electrical conductivities in DMSO, are summarized in Table 6. The electrical conductivities measured in DMSO deviate slightly from zero, indicating that the dinuclear structure partially decomposes in this solvent. The unique redox process observed around -0.22 V is assigned to the Cu(II)→Cu(III) oxidation of the {CuL} site. The corresponding process for the mononuclear Cu(II) precursor, [Me₄N]₂[CuL]·H₂O, is observed at -0.207 V, indicating that the redox potential is substantially affected by the formation of a dinuclear structure: the Cu(III) oxidation state is destabilized through the formation of a dinuclear structure. The quasi-reversible process observed at -1.570 V for [CuLNi(bpy)₂]·1.5H₂O and -1.907 V for [CuLCo(bpy)₂]·1.5H₂O is assigned to the M(II)→M(I) reduction of the {M(bpy)₂} site.

Concluding Remarks. This study revealed that the dianionic copper(II) complexes with 1,2-bis(2-hydroxybenz-amido)benzene and the analogous H₄L' ligand can function as multidentate ligand-complexes at the phenoxo and amido oxygen atoms. (1) The molar ratio of the bpy terminal capping ligand against [CuL]²⁻ and the second metal ion in the reaction mixture determines whether or not the amido oxygen atom participates in an additional bridge. When the second metal ion is coordinatively saturated by the two phenoxo-oxygen atoms and the two bpy ligand, that is, K₂[CuL], metal(II) acetate, and bpy were mixed in methanol with the 1 : 1 : 2 molar ratio, a di- μ -phenoxo-bridged dinuclear complex is obtained. When the second metal ion is coordinated by two phenoxo-oxygen atoms and one bpy ligand, that is, K₂[CuL], metal(II) acetate, and bpy were mixed in methanol with the 1 : 1 : 1 molar ratio, its available coordination site induces dimerization of two dinuclear molecules through coordination of one amido oxygen of the adjacent unit to the second metal ion yielding a cyclic di- μ -phenoxo- μ -amido-bridged tetranuclear complex. (2) The preferable coordination geometry around the second metal ion as well as the recrystallization solvent affect the nuclearity. Copper(II) and zinc(II) ions in the second metal ion site prefer a penta-coordinated geometry rather than a hexa-coordinated geometry. When [CuLZn(bpy)₂]·1.5H₂O (**3**) was recrystallized from DMF, one bpy molecule of **3** was removed to produce cyclic tetranuclear [CuLZn(bpy)₂]·2DMF (**3'**). When **3** was recrystallized from DMSO, which is a stronger donating ligand, **3**

was obtained. In the absence of a terminal capping ligand, the two amido oxygen atoms and the two phenoxo oxygen atoms might all participate in bridges, possibly yielding an extended multi-dimensional structure. A study along this line is now in progress in our laboratories.

The work was supported by Monbuscho International Scientific Research Program (No. 10044089 "Joint Research") and by a Grant-in-Aid for Scientific Research on Priority Area (No. 10149101 "Metal-assembled Complexes").

References

- 1) a) O. Kahn, "Molecular Magnetism," VCH Verlagsgesellschaft, Weinheim, Germany (1993); b) Edited by D. Gatteschi, O. Kahn, J. S. Miller, and F. Palacio, "Magnetic Molecular Materials," NATO ASI Series E, Vol. 198, Kluwer Academic, Dordrecht, Holland (1991); c) O. Kahn, *Struct. Bonding*, **67**, 89 (1987); d) A. Gleizes and M. Verdagner, *J. Am. Chem. Soc.*, **103**, 7373 (1981).
- 2) a) U. Bossek, T. Weyhermuller, K. Weighardt, B. Nuber, and J. Weiss, *J. Am. Chem. Soc.*, **112**, 6387 (1990); b) Y. Naruta, M. Sasayama, and T. Sasaki, *Angew. Chem., Int. Ed. Engl.*, **33**, 1839 (1994); c) N. Strater, T. Klabunde, P. Tucker, H. Witzel, and B. Krebs, *Science*, **268**, 1489 (1995); d) M. P. Egloff, P. T. W. Cohen, P. Reinemer, and D. Barford, *J. Mol. Biol.*, **254**, 942 (1995).
- 3) a) O. Kahn, J. Galy, Y. Journaux, and I. Morgenstern-Badarau, *J. Am. Chem. Soc.*, **104**, 2165 (1982); b) T. Aono, H. Wada, Y. Aratake, N. Matsumoto, H. Okawa, and Y. Matsuda, *J. Chem. Soc., Dalton Trans.*, **1996**, 25; c) M. Yonemura, Y. Matsumura, H. Furutachi, M. Ohba, and H. Okawa, *Inorg. Chem.*, **36**, 2711 (1997); d) H. Okawa, J. Nishio, M. Ohba, M. Tadokoro, N. Matsumoto, M. Koikawa, S. Kida, and D. E. Fenton, *Inorg. Chem.*, **32**, 2949 (1993); e) D. E. Fenton and R. L. Lintvedt, *J. Am. Chem. Soc.*, **100**, 6367 (1978); f) W. Mazurek, K. J. Berry, K. S. Murry, M. J. O'Connor, S. J. Snow, and A. G. Wedd, *Inorg. Chem.*, **21**, 3071 (1982); g) R. R. Gagné, C. L. Spiro, T. J. Smith, C. A. Hamann, W. R. Thies, and A. K. Shiemke, *J. Am. Chem. Soc.*, **103**, 4073 (1981); h) D. G. McCollum, G. P. A. Yap, A. L. Rheingold, and B. Bosnich, *J. Am. Chem. Soc.*, **118**, 1365 (1996); i) L. K. Thompson, S. S. Tandon, and M. E. Manuel, *Inorg. Chem.*, **34**, 2356 (1995); j) S. Mohanta, K. K. Nanda, R. Werner, W. Haase, A. K. Mukherjee, S. K. Dutta, and K. Nag, *Inorg. Chem.*, **36**, 4656 (1997).
- 4) a) C. T. Brewer, G. Brewer, G. Jameson, P. Kamaras, L. May, and M. Rapta, *J. Chem. Soc., Dalton Trans.*, **1995**, 37; b) C. A. Koch, C. A. Reed, G. Brewer, N. P. Rath, W. R. Scheidt, G. P. Gupta, and G. Lang, *J. Am. Chem. Soc.*, **111**, 7645 (1989); c) J.-P. Costes, F. Dahan, and J.-P. Laurent, *J. Chem. Soc., Dalton*

- Trans.*, **1989**, 1017; d) N. Matsumoto, T. Akui, H. Murakami, J. Kanesaka, A. Ohyoshi, and H. Okawa, *J. Chem. Soc., Dalton Trans.*, **1988**, 1021; e) N. Matsumoto, M. Mimura, Y. Sunatsuki, S. Eguchi, Y. Mizuguchi, H. Miyasaka, and T. Nakashima, *Bull. Chem. Soc. Jpn.*, **70**, 2461 (1997); f) T. Nozaki, H. Ushio, G. Mago, N. Matsumoto, H. Okawa, Y. Yamakawa, T. Anno, and T. Nakashima, *J. Chem. Soc., Dalton Trans.*, **1994**, 2339; g) N. Matsumoto, Y. Mizuguchi, G. Mago, S. Eguchi, H. Miyasaka, T. Nakashima, and J.-P. Tuchagues, *Angew. Chem., Int. Ed. Engl.*, **36**, 1860 (1997); h) J.-P. Costes, F. Dahan, and J.-P. Laurent, *J. Chem. Soc., Dalton Trans.*, **1989**, 1017; i) J.-P. Costes, F. Dahan, A. Dupuis, and J.-P. Laurent, *Inorg. Chem.*, **35**, 2400 (1996); j) N. B. O'Bryan, T. O. Maier, I. C. Paul, and R. Drago, *J. Am. Chem. Soc.*, **95**, 6640 (1973); k) V. Baron, B. Gillon, O. Plantevin, A. Cousson, C. Mathoniere, O. Kahn, A. Grand, L. Öhrström, and B. Delley, *J. Am. Chem. Soc.*, **118**, 11822 (1996); l) J. Larionova, S. A. Chavan, J. V. Yakhmi, A. G. Frøystein, J. Sletten, C. Sourisseau, and O. Kahn, *Inorg. Chem.*, **36**, 6374 (1997); m) Y. Pei and O. Kahn, *J. Am. Chem. Soc.*, **108**, 3143 (1986); n) E. Sinn and M. Harris, *Coord. Chem. Rev.*, **4**, 391 (1969); o) R. Ruiz, M. Julve, J. Faus, F. Lloret, M. C. Muñoz, Y. Journaux, and C. Bois, *Inorg. Chem.*, **36**, 3434 (1997); p) S. W. Gordon-Wylie, E. L. Bominaar, T. J. Collins, J. M. Workman, B. L. Claus, R. E. Patterson, S. A. Williams, B. L. Conklin, F. T. Yee, and S. T. Weintraub, *Chem. Eur. J.*, **1**, 528 (1995).
- 5) N. Matsumoto, M. Ohba, M. Mitsumi, K. Inoue, Y. Hashimoto, and H. Okawa, *Mol. Cryst. Liq. Cryst.*, **233**, 299 (1993).
- 6) a) O. Kahn, Y. Pei, M. Verdauger, J. P. Renard, and J. Sletten, *J. Am. Chem. Soc.*, **110**, 782 (1988); b) Y. Pei, M. Verdager, O. Kahn, J. Sletten, and J. P. Renard, *Inorg. Chem.*, **26**, 138 (1987).
- 7) K. Nakatani, J. Y. Carriat, Y. Journaux, O. Kahn, F. Lloret, J. P. Renard, Y. Pei, J. Sletten, and M. Verdager, *J. Am. Chem. Soc.*, **111**, 5739 (1989).
- 8) a) Y. Sunatsuki, M. Nakamura, N. Matsumoto, and F. Kai, *Bull. Chem. Soc. Jpn.*, **70**, 1851 (1997); b) Y. Sunatsuki, M. Mimura, T. Shimada, F. Kai, and N. Matsumoto, *Bull. Chem. Soc. Jpn.*, **71**, 167 (1998); c) Y. Sunatsuki, R. Hirata, Y. Motoda, M. Nakamura, N. Matsumoto, and F. Kai, *Polyhedron*, **16**, 4105 (1997); d) A. Stassinopoulous, G. Schulte, G. C. Papaefthymiou, and J. P. Caradonna, *J. Am. Chem. Soc.*, **113**, 8686 (1991).
- 9) D. Perrin and W. L. F. Armarego, "Purification of Laboratory Chemicals," 3rd ed, Pergamon, Oxford (1988).
- 10) a) C. Anson, T. J. Collins, S. L. Gipson, J. T. Keech, T. E. Krafft, and G. T. Peake, *J. Am. Chem. Soc.*, **108**, 6593 (1986); b) N. O. O'Bryan, T. O. Maier, I. C. Paul, and R. S. Drago, *J. Am. Chem. Soc.*, **95**, 6640 (1973).
- 11) E. A. Boudreaux and L. N. Mulay, "Theory and Applications of Molecular Paramagnetism," Wiley, New York (1976), p. 491; A. Earnshaw, "Introduction to Magnetochemistry," Academic Press, New York (1968).
- 12) G. M. Sheldrick, "SHELXS86 A program for X-ray crystal structure determination," University of Cambridge (1986); P. T. Beurskens, G. Admiraal, G. Beurskens, W. P. Bosman, S. Garcia-Granda, R. O. Gould, J. M. M. Smits, and C. Smykalla, "DIRDIF92 The DIRDIF Program System, Technical Report of the Crystallography Laboratory," University of Nijmegen, The Netherlands (1992).
- 13) D. C. Creagh and W. J. McAuley, "International Tables for Crystallography," ed by A. J. C. Wilson, Kluwer Academic Publishers, Boston (1992), Vol. C, Table 4.2.6.8, pp. 219—222; D. T. Cromer and J. T. Waber, "International Tables for X-Ray Crystallography," The Kynoch Press, Birmingham, England (1974), Vol. IV, Table 2.2A.
- 14) D. C. Creagh and J. H. Hubbel, "International Tables for Crystallography," ed by A. J. C. Wilson, Kluwer Academic Publishers, Boston (1992), Vol. C, Table 4.2.4.3, pp. 200—206; D. C. Creagh and W. J. McAuley, "International Tables for Crystallography," ed by A. J. C. Wilson, Kluwer Academic Publishers, Boston (1992), Vol. C, Table 4.2.6.8, pp. 219—222.
- 15) "teXsan: Crystal Structure Analysis Package," Molecular Structure Corporation (1985 & 1992).
- 16) A. W. Addison, T. N. Rao, J. Reedijk, J. van Rijn, and G. C. Verschoor, *J. Chem. Soc., Dalton Trans.*, **1984**, 1349.
- 17) a) A. O. Ginsberg and M. E. Lines, *Inorg. Chem.*, **11**, 2289 (1972); b) O. Kahn, *Struct. Bonding*, **68**, 89 (1989).
- 18) a) S. L. Lambert, C. L. Spiro, R. R. Gagne, and D. N. Hendrickson, *Inorg. Chem.*, **21**, 68 (1982); b) O. Kahn, P. Tola, and H. Coudanne, *Chem. Phys.*, **42**, 355 (1979); c) N. Matsumoto, K. Inoue, M. Ohba, H. Okawa, and S. Kida, *Bull. Chem. Soc. Jpn.*, **65**, 2283 (1992).
- 19) a) W. E. Hatfield and G. W. Inman, *Inorg. Chem.*, **8**, 1376 (1969); b) G. Kolks, S. J. Lippard, J. V. Waszczak, and H. R. Lillienthal, *J. Am. Chem. Soc.*, **104**, 717 (1982); c) C. Fukuhara, K. Tsuneyoshi, K. Katsura, N. Matsumoto, S. Kida, and M. Mori, *Bull. Chem. Soc. Jpn.*, **62**, 3939 (1989).